

Article

Theoretical Investigation on Rare Earth Elements of Y, Nd and La Atoms' Adsorption on the Kaolinite (001) and (00 $\bar{1}$) Surfaces

Jian Zhao ^{1,2}, Zheng Wang ^{1,2,*}, Wei Gao ^{1,2}, Yi-Fei Wang ^{1,2} and Bo-Wen Huang ^{1,2}

¹ State Key Laboratory of Geomechanics and Deep Underground Engineering, China University of Mining and Technology, Beijing 100083, China; zhaojian@cumtb.edu.cn (J.Z.); gaow@student.cumtb.edu.cn (W.G.); wyfya@student.cumtb.edu.cn (Y.-F.W.); berwyn@student.cumtb.edu.cn (B.-W.H.)

² School of Mechanics and Civil Engineering, China University of Mining and Technology, Beijing 100083, China

* Correspondence: wangz9696@student.cumtb.edu.cn; Tel.: +86-1583-757-2714

Abstract: With the growing demand of rare earth elements, the recovery of rare earth elements is a major issue for researchers in related fields. Adsorption technology is one of the most effective and popular recovery methods. Therefore, the adsorption mechanism of Yttrium (Y), Neodymium (Nd), and Lanthanum (La) atoms on the kaolinite (001) and (00 $\bar{1}$) surfaces was examined by density functional theory (DFT). The most stable adsorption sites on the kaolinite (001) surface for Y atoms was the bridge site, and the hollow site was the most favorable adsorption site for Nd and La atoms with high adsorption energy. However, the adsorption energies of kaolinite (00 $\bar{1}$) surface sites for Y, Nd, and La atoms were much lower than the (001) surface sites, indicating that the adsorption capability of the hydroxylated (001) surface is stronger. The effects of coverage on adsorption position, energy, and structures were entirely investigated on top, bridge, and hollow sites of the kaolinite (001) surface from 0.11 to 1.0 monolayers (ML). The adsorption energy of Y, Nd, and La atoms on three kinds of sites increased with increasing of the coverage implied the stronger capability of surface adsorption. The recovery capability of kaolinite for the rare earth atoms was in the order of La > Nd > Y. The changes in the atomic structure, charge density, and electron density of states for Y, Nd, and La/kaolinite (001) before and after adsorption were also analyzed in depth.

Keywords: clay minerals; kaolinite; rare earth elements; adsorption; density functional theory



Citation: Zhao, J.; Wang, Z.; Gao, W.; Wang, Y.-F.; Huang, B.-W. Theoretical Investigation on Rare Earth Elements of Y, Nd and La Atoms' Adsorption on the Kaolinite (001) and (00 $\bar{1}$) Surfaces. *Minerals* **2021**, *11*, 856. <https://doi.org/10.3390/min11080856>

Academic Editor: Jordi Ibanez-Insa

Received: 21 June 2021

Accepted: 6 August 2021

Published: 9 August 2021

Publisher's Note: MDPI stays neutral with regard to jurisdictional claims in published maps and institutional affiliations.



Copyright: © 2021 by the authors. Licensee MDPI, Basel, Switzerland. This article is an open access article distributed under the terms and conditions of the Creative Commons Attribution (CC BY) license (<https://creativecommons.org/licenses/by/4.0/>).

1. Introduction

As a strategic resource, rare earth elements (REEs) have always been used in the fields of metallurgy, medicine, the chemical industry, and agriculture [1,2]. The improved technology has created a growing demand for REEs. Recently, there has been an increased recognition that the recovery of REEs is of great significance owing to the consideration of ensuring the current and future supply of REEs [3]. It is well known that various approaches (e.g., biological treatment, chemical precipitation, and adsorption) have been geared towards the recovery of REEs [4,5]. Araki et al. [6] and Alakhras et al. [7] used the surface template polymerization technique to create an adsorbent with high selectivity for lanthanides. Chio et al. [8] used radiation-induced grafting of acrylic acid (AAc) onto polyethylene (PE) films to adsorb Lanthanide. However, the adsorption ability of the above materials was weak in practical application. Clay minerals are attractive in comparison with the above materials because they are widespread, easily mined, and inexpensive [9,10]. Some studies have indicated that clay minerals can show good adsorption behavior for metals, organic substances, and other materials [11,12]. Consequently, clay minerals were used as adsorbents for the recovery of REEs from aqueous wastes [13,14].

Kaolinite is a widespread and abundant clay [15,16] that has always been regarded as a potential adsorbent because of its cation exchange capacity and higher adsorption capacity. Therefore, many researchers have carried out a host of experimental studies to use kaolinite

as an adsorbent for the recovery of REEs. In 1984, Laufer et al. [17] studied the adsorption behavior of Cerium (IV) from ceric ammonium nitrate using natural and modified kaolinite, and the result implied that Ce could be adsorbed either as a monomeric species or as a polymeric hydroxy cation. Aja et al. [18] investigated the recovery of Nd onto kaolinite, and the results showed that kaolinite has a large capability for Nd atoms. Coppin et al. [19] discussed the adsorption behavior of REEs on kaolinite, and they found that the adsorption capacity of REEs was large in comparison with light rare earth elements due to selective adsorption. Wan et al. [20] studied kaolinite as an adsorbent to absorb the rare earth ions Y, Ga, Nd, and La in highly acidic solution and found that heavy REEs can be enriched in kaolinite under corrosive acid. Xiao et al. [21] investigated the adsorption thermodynamics of REEs on kaolinite, and the results implied that the adsorption properties of La, Nd, and Y on kaolinite conform to the Langmuir isotherm model. The above experimental results clarified that kaolinite can be used as a favorable and economical adsorbent to recycle REEs, and its adsorption effect is remarkable. However, the above studies on the adsorption mechanism at an atomic level were not clear due to the limitation of the experiments. The geometry information about how the REE atoms adsorbed on the kaolinite and other interaction behavior at an atomic level was still worthy of further exploration.

Over the decades, multiple computer simulations based on the DFT method have been proved scientific and credible for studying adsorption at a molecular level [22,23]. For instance, Zhang et al. [24] studied Ca and K atoms adsorbed on the kaolinite surface by DFT calculations and the Monte Carlo method. The adsorption behavior of CO₂ on a pristine or doped kaolinite (001) surface was also studied by the DFT method [25]. Especially, Lanthanum (La), Neodymium (Nd), and Yttrium (Y) have caught much attention with their increasing applications in advanced new materials for their unique physical and chemical properties [26,27] and high partition in the earth's crust [28]. The present paper was written from the perspective of the microscopic level, and Y, Nd, and La atoms were chosen as the main research object to analyze the adsorption characteristics of REEs on kaolinite, which could provide theoretical support for the adsorption of Y, Nd, and La atoms on the hydroxylated (001) surface and the tetrahedral (00 $\bar{1}$) surface. Moreover, the binding positions, binding energies, and the electron transfer between REEs and atoms of kaolinite were also obtained.

2. Method of Calculations

The adsorption behavior and geometric configuration of Y, Nd, and La atoms were calculated by the Vienna ab-initio simulation package [29] based on density functional theory (DFT). The generalized gradient approximation (GGA) formulation with the Perdew–Burke–Ernzerhof (PBE) functional was used to calculate the exchange and correlation functional between electrons. REE electrons were treated using the effective core potentials, which introduce some degree of relativistic correction into the core of REE elements in calculation. Using a plane-wave pseudopotential and periodic boundary conditions to solve the Kohn–Sham DFT equation, the electron was treated by quantum mechanics. The electron–ion interaction was described by the project augmented wave (PAW) method, which takes the exact shape of the valence wave functions into account [30]. O 2s²p⁴, H 1s¹, Al 3s²3p², Si 3s²3p², Y 4d¹5s², Nd 4f⁴6s², and La 5d¹6s² were regarded as the valence electrons. The selection of the k-point adopts the Monkhorst–Pack scheme with the Γ point as the center. In the process of structural optimization and static calculation, a (3 × 3 × 1) k-point grid was used for p (2 × 2) and p (3 × 3) surface cells. The cutoff energy of plane-wave basis was set to 400 eV. The criterion of energy convergence in the optimization of atomic geometries and SCF energy was set to 1 × 10^{−4} eV, and 0.02 eV/Å for the atomic force.

The existing experimental data [31–33] and calculated results [34–40] of kaolinite with the crystal structure of Al₂Si₂O₅(OH)₄ often consist of two different surfaces of aluminosilicate as a perfect 1:1 layer structure [34,41]. One side consists of a gibbsite-type sheet and the other is a silica sheet [42]. In the present paper, the optimal structural

parameters for bulk kaolinite were as follows: $a = 5.155 \text{ \AA}$, $b = 5.155 \text{ \AA}$, $c = 7.405 \text{ \AA}$, $\alpha = 75.14^\circ$, $\beta = 84.12^\circ$ and $\gamma = 60.18^\circ$, corresponding with the experimental results and the other calculated data [43]. The kaolinite surface can be divided into the hydroxylated (001) surface and the tetrahedral ($00\bar{1}$) surface. The kaolinite (001) and ($00\bar{1}$) surfaces modeled a periodically repeated slab composed of six kaolinite layers with a vacuum thickness of 20 \AA , respectively. REE atoms were placed on the hydroxylated (001) surface and the tetrahedral ($00\bar{1}$) surface, respectively. Dipole correction and spin polarization were considered to minimize the possible inaccuracies between periodic images of the slabs. According to kaolinite surface symmetry, different initial positions (top site (T_1 – T_3); bridge site (B_1 – B_2); hollow site (H_1 – H_4)) on the kaolinite (001) and (top site (T_2 – T_6); bridge site (B_3 – B_5); hollow site (H_5)) on the ($00\bar{1}$) surfaces would be examined. Four hollow, two bridge, and three top adsorption sites on the kaolinite (001) surface and one hollow, three bridge, and three top adsorption sites on the kaolinite ($00\bar{1}$) surface were examined, as shown in Figure 1. Especially, we used surface unit cells of p (3×3) to calculate adsorbate coverages of 0.11 and 0.33 ML, and the coverages of 0.25, 0.5, 0.75, and 1.0 ML were calculated using surface unit cells of p (2×2).

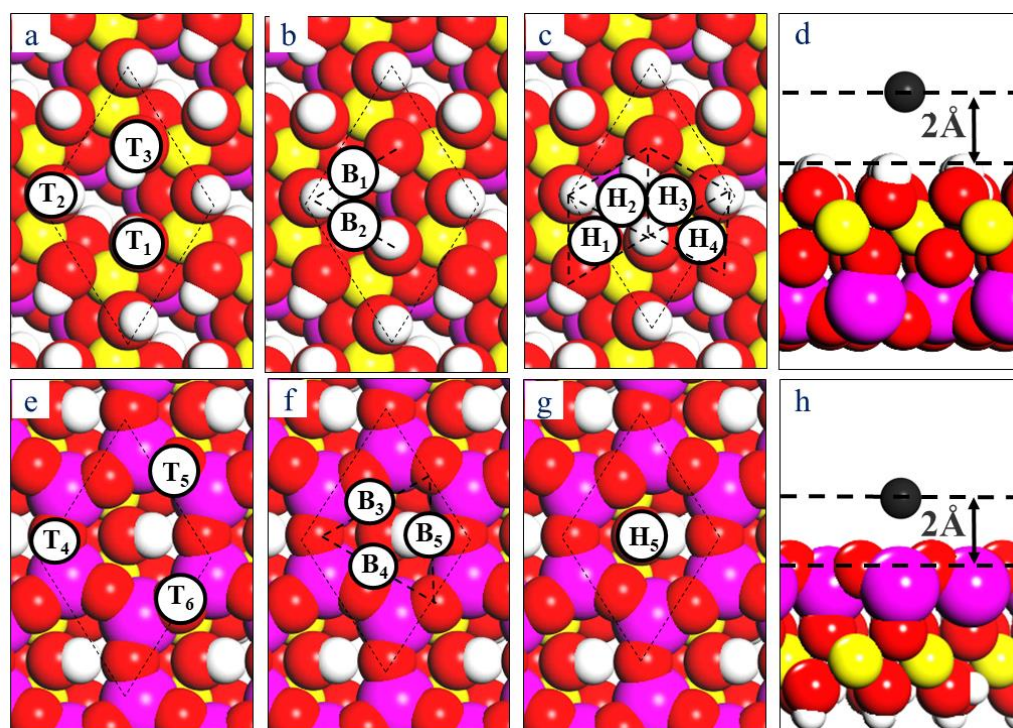


Figure 1. (a–c) Top view of kaolinite (001) surface with three top adsorption sites (T_1 – T_3), two bridge adsorption sites (B_1 – B_2), and four hollow adsorption sites (H_1 – H_4). Top view of kaolinite ($00\bar{1}$) surface with (e) three top adsorption sites (T_4 – T_6), (f) three bridge adsorption sites (B_3 – B_5), and (g) one hollow adsorption site (H_5). Side view of the initial relative position model between Y (Nd or La) and kaolinite (001) surface (d) and ($00\bar{1}$) surface (h) before adsorption. Here, white spheres, red spheres, yellow spheres, purple spheres, and dim grey spheres represent hydrogen, oxygen, aluminum, and silicon, Y (Nd or La) atom, respectively.

3. Results and Discussions

The adsorption energy (E_{ads}) was often used to evaluate the adsorption stability of REE atoms on kaolinite, and E_{ads} was the average adsorption energy of REE atoms on the kaolinite (001) and ($00\bar{1}$) surface, defined as the following equation:

$$E_{\text{ads}}(\Theta) = \frac{1}{N_{\text{REEs}}} [E_{\text{substrate}} + N_{\text{REEs}} E_{\text{REEs}} - E_{\text{REEs/substrate}}] \quad (1)$$

Here, N_{REE} was the number of REE (REEs = Y, Nd, and La) adatoms adsorbed on the slab at the considered coverage Θ (Θ was defined as the ratio of the number of adsorbed atoms to the optimum adsorption sites on the surface of kaolinite) [44]. $E_{\text{REEs/substrate}}$, $E_{\text{substrate}}$, and E_{REEs} were the total energy of the adsorption system of REE atoms and the kaolinite surface, the clean kaolinite surface, and free REE atoms, respectively. The greater the absolute value of adsorption energy, the more stable the adsorption, according to the above formula. All three kinds of high-symmetry adsorption sites of kaolinite (001) and (00 $\bar{1}$) surfaces were considered, respectively, as shown in Figure 1.

As shown in Figure 2a–d, the three highly symmetrical adsorption sites were the stable site of Y, Nd, and La atoms adsorbed on the kaolinite (001) surface. According to the calculated results, the bridge site was the favorite adsorption site for Y atoms, followed in the order of reducing stability by the hollow and top site. Meanwhile, the most stable among all possible adsorption sites for Nd atoms was the hollow site, followed by the bridge and top site of the kaolinite (001) surface. The hollow site was also the most stable adsorption site for La atoms, followed by the top site and bridge site. We calculated the E_{ads} (Table 1) of Y, Nd, and La atoms on three kinds of adsorption sites of the kaolinite (001) surface at different coverages (from 0.11 to 1 ML). As listed in Table 1, the adsorption energy of the bridge site was always larger than the top and hollow site for Y atoms. The minimum and maximum adsorption energies of Y atoms on the three kinds of adsorption sites were at 0.11 ML and 1.0 ML, respectively. The adsorption energy increased with increasing the coverage of Y atoms at three kinds of adsorption sites. Meanwhile, the hollow site was more stable than the top and bridge sites for Nd and La atoms from 0.11 to 1.0 ML. The adsorption energies of Nd and La atoms on top, bridge, and hollow sites ranged from 94.2 to 166.3 kJ/mol, 126.9 to 189.4 kJ/mol, 166.3 to 227.8 kJ/mol, 151.91 to 221.1 kJ/mol, and 168.2 to 232.7 kJ/mol, respectively. Similarly, the low coverage ($\Theta = 0.11$ ML) had the minimum adsorption energy and the high coverage ($\Theta = 1.0$ ML) had the maximum adsorption energy. The quality for Y, Nd, and La atoms on three kinds of adsorption sites displayed a modestly increasing tendency from 0 to 1.0 ML, respectively. In the coverage range of $0 < \Theta \leq 1.0$ ML, the increasing adsorption energy implied a tendency to form REE islands on the kaolinite (001) surface. The adsorption energy indicates the interaction between the oxygen atom in the adsorption active center and the adsorbed rare earth atom. The higher the adsorption energy, the easier the atom is adsorbed [20,45]. The above results showed that kaolinite can be used as an adsorbent to recover rare earth atoms, and the order of recovery ability of different rare earth atoms on kaolinite was La > Nd > Y.

Table 1. The adsorption energy E_{ads} (kJ/mol) of REEs (REEs = Y, Nd, and La) adsorbed on the (001) surface of kaolinite at different coverages.

Site	Y			Nd			La		
	Top	Bridge	Hollow	Top	Bridge	Hollow	Top	Bridge	Hollow
ML 0.11	109.6	137.5	108.6	94.2	126.9	132.7	166.3	151.9	168.2
ML 0.25	128.8	141.3	128.8	103.8	140.4	141.3	169.2	154.8	172.1
ML 0.33	129.8	147.1	132.7	146.1	149.0	151.9	170.2	159.6	176.0
ML 0.5	146.1	153.8	137.5	152.9	148.1	155.8	221.1	180.8	226.9
ML 0.75	152.9	155.8	146.1	156.7	159.6	176.9	224.0	215.4	226.0
ML 1.0	156.7	165.4	149.0	166.3	164.4	189.4	227.8	221.1	232.7

Furthermore, the adsorption energy and geometric equilibrium of rare earth element atoms onto the (00 $\bar{1}$) surface of kaolinite were also investigated. With respect to the Y atom adsorbed on the (00 $\bar{1}$) surface, a Y atom adsorbed on the bridge and hollow adsorption site was energetically stable with the adsorption energy of 41.3 and 42.3 kJ/mol, respectively (Figure 2e,f). Similarly, La and Nd atoms adsorbed on three adsorption sites had an adsorption energy of below 48.1 kJ/mol, as listed in Table 2. Compared with Table 1, the adsorption energy of kaolinite (00 $\bar{1}$) surface for REE atoms was weak. Consequently, the

adsorption characteristics of REE atoms on the (001) surface of kaolinite with different coverages were mainly discussed in the present paper.

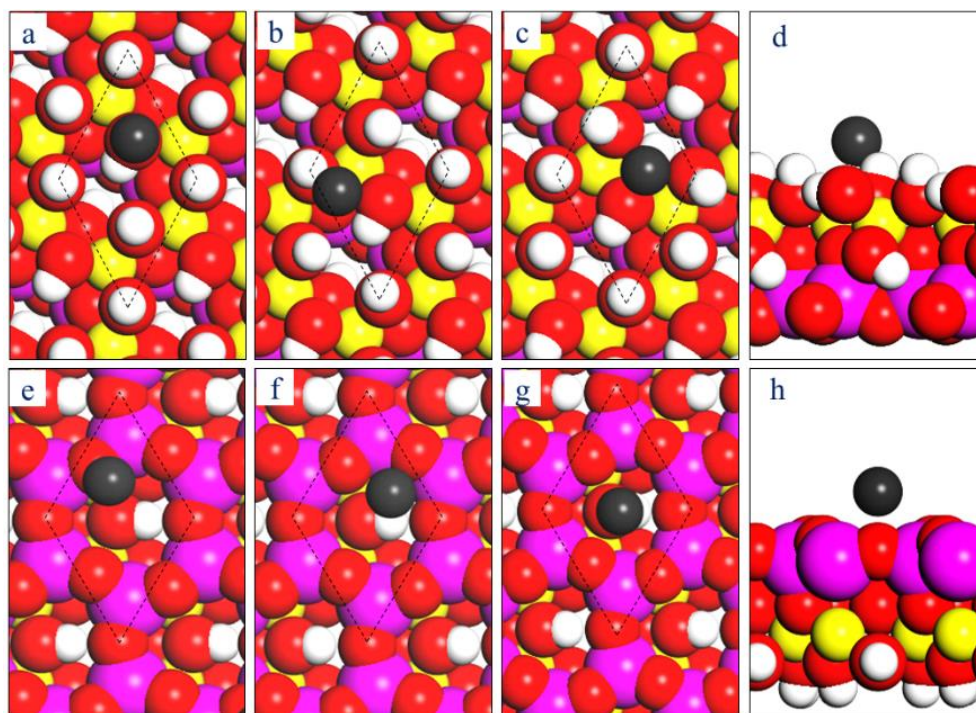


Figure 2. Top (a) and side (d) view of adsorbed Y (Nd or La) atoms on the top sites of kaolinite (001) surface, adsorbed Y (Nd or La) atoms on the (b) bridge sites, and adsorbed Y (Nd or La) atoms on the (c) hollow sites. Top (e) and side (h) view of Nd atoms adsorbed on the top site (Figure S1) of kaolinite (00 $\bar{1}$) surface, adsorbed La (Y) atoms on the (f) bridge sites and adsorbed Nd (Y) atoms on the (g) hollow site. Here, adsorbed Y, Nd, and La atoms are colored dim grey for clarity.

Table 2. The adsorption energy E_{ads} (kJ/mol) of REEs (REEs = Y, Nd, and La) adsorbed on the (00 $\bar{1}$) surface of kaolinite.

Site	Y		Nd		La	
	Bridge	Hollow	Top	Hollow	Bridge	Hollow
E_{ads}	41.3	42.3	36.5	43.2	43.2	48.1

Table 3 shows the calculated geometries for REE atoms' adsorption on the optimal adsorption sites of the kaolinite (001) surface at coverages of 0.25, 0.5, 0.75, and 1.0 ML, including the vertical height $h_{\text{REEs-Al}}$ between the adsorbed REE atoms and the aluminum atomic layer on the kaolinite (001) surface, the average REE–O bond length R_a , as well as the changed ratio of interlayer distances (Δd_{ij}). The changes in Δd_{ij} were calculated according to the formula $\Delta d_{ij} = (d_{ij} - d_0) / d_0$ [46], where d_{ij} was the distance between the i th and j th layers of kaolinite along the [1] vector direction after relaxation, and d_0 was the i th and j th layers in initial kaolinite. As listed in Table 3, the vertical height $h_{\text{REEs-Al}}$ of REE atoms to the kaolinite (001) surface decreased gradually with the increase in coverage at all types of adsorption sites, and we found that the $h_{\text{REEs-Al}}$ of the Y adsorbed on the bridge site and the La and Nd adsorbed on the hollow site were shorter than the other adsorption sites at all coverages ($0 < \Theta \leq 1.0$ ML), respectively. The shorter $h_{\text{REEs-Al}}$ means stable adsorption. The above results meant the binding site was more stable than the other two kinds of adsorption sites for Y atoms and the hollow site had a larger capability than the other two kinds of sites for La and Nd atoms. Finally, the significant changes in the interlayer distances of the substrate kaolinite were caused by REE atoms adsorbing on the

(001) surface. In addition, Table 3 shows the bond length R_a of REE atoms between O atoms of the kaolinite (001) surface at different coverages. After Y atoms were adsorbed on the bridge site, the Y–O bond length varied from 2.49 Å to 2.45 Å at different coverages, and the shorter bond length means it is more stable than the other two kinds of sites for Y atoms. When Nd atoms were adsorbed on the hollow site, the bond lengths of Nd–O varied from 2.44 Å to 2.42 Å in the coverage range of $0 < \Theta \leq 1.0$ ML. Similarly, the La–O bond length changed from 2.45 Å to 2.42 Å when increasing the coverage range. The above results mean the hollow site has more adsorption capability for Nd and La atoms. Meanwhile, the data of bond lengths indicated the length recovery of the kaolinite (001) surface for three REE atoms with increasing coverage, which is consistent with the adsorption energy. In particular, when REE atoms were adsorbed on the three high adsorption sites, the value of Δd_{12} was positive with increasing coverage, which meant that the layer spacing between the first and the second layer of the kaolinite (001) surface expanded and became larger with increasing Θ . However, the value of Δd_{23} was from 2.12% to -0.55% and 0.21 to -7.14% with increasing Θ values, respectively, which meant the second interlayer contracted and became smaller with increasing Nd coverage. Interestingly, the value of Δd_{23} decreased from 3.87% to -4.18% , and then increased to 1.63%, indicating that the space between the second and third layers first contracted and then expanded for Y in the hollow site. The interlayer spacing change of kaolinite reflects the change of H-bonding between layers caused by the adsorption of REE atoms, which makes the structure of kaolinite relax back to its ‘ideal’ bulk value.

Table 3. The vertical height ($h_{\text{REES-AI}}$), the bond length (R_a), and the changed ratio of interlayer distances (Δd_{12} and Δd_{23}) after REE atoms were adsorbed on kaolinite (001) surface.

Phase	Θ	Y			Nd			La		
		Top	Bridge	Hollow	Top	Bridge	Hollow	Top	Bridge	Hollow
$h_{\text{REES-AI}}$ (Å)	0.25 ML	3.42	3.32	3.44	3.43	3.24	3.15	3.33	3.34	3.10
	0.5 ML	3.42	3.29	3.43	3.42	3.17	3.09	3.32	3.34	3.08
	0.75 ML	3.39	3.15	3.42	3.42	3.13	3.07	3.1	3.26	2.98
	1.00 ML	3.38	3.10	3.42	3.40	3.10	2.95	2.92	3.26	2.93
R_a (Å)	0.25 ML	2.57	2.49	2.52	2.49	2.45	2.44	2.45	2.49	2.45
	0.5 ML	2.53	2.47	2.53	2.49	2.45	2.44	2.45	2.48	2.43
	0.75 ML	2.50	2.43	2.42	2.48	2.44	2.42	2.42	2.46	2.42
	1.00 ML	2.57	2.45	2.59	2.48	2.43	2.42	2.45	2.52	2.42
Δd_{12} (%)	0.25 ML	1.95	2.11	1.83	2.10	2.23	2.23	1.83	1.81	1.95
	0.5 ML	3.45	3.21	2.53	2.13	2.10	2.11	2.59	2.34	1.86
	0.75 ML	2.23	4.10	2.48	3.84	3.85	2.35	2.70	3.18	3.10
	1.00 ML	4.82	3.70	2.68	4.05	2.11	3.26	3.70	2.52	2.88
Δd_{23} (%)	0.25 ML	3.77	1.73	3.87	2.12	0.21	1.98	3.36	3.22	2.25
	0.5 ML	1.52	1.93	5.16	2.15	0.71	2.02	2.04	-6.72	1.25
	0.75 ML	10.2	7.14	-4.18	-0.32	-5.32	2.25	-3.82	1.01	0.81
	1.00 ML	12.6	12.34	1.63	-0.55	-7.14	1.62	2.90	1.25	0.81

To investigate the electron transfer between REE atoms and O atoms of the kaolinite surface, the Bader charge and the different charge densities of the kaolinite surface before and after Y atom adsorption at $\Theta = 0.25$ ML were also calculated and analyzed. Table 4 lists the change in Bader’s charge for the REE adatoms and O atoms on the (001) surface of kaolinite. Negative (positive) values meant the loss (gain) of electrons. O₁, O₂, O₃, O₄, O₅, and O₆ were the O atoms connected to the REE atoms adsorbed at the top, bridge, and hollow sites, respectively. It is obvious that the charge transferred from REE atoms to O atoms of the kaolinite (001) surface. The more electrons gained and lost means the stronger the bonding effect. Meanwhile, the data of Bader’s charge indicated that the bonding effect was the strongest as Y was adsorbed at the bridge site, which was consistent with the adsorption energy. The three-dimensional (3D) electron density difference map, as

shown in the insets to Figure 3, visualized the electron density transfer between adsorbate and adsorbate after adsorption. The blue and yellow areas represent the accumulation and depletion of electron density upon bonding, respectively. According to Figure 4a, the electron density around Y adatoms increased while the electron density around O atoms and H atoms of the surface depleted. This phenomenon indicated that the electron density is transferred from the O and H atoms on the surface of kaolinite to Y atoms, resulting in the formation of a covalent bond between Y and the kaolinite surface. The 3D differential density map of the bridge and hollow site was basically the same as that of the top site. Therefore, the above analysis was also applicable to the bridge and hollow site. Similarly, the charge transferred between the adsorbate and the substrate was consistent with the Bader charge difference analysis.

Table 4. Change in Bader’s charge for the REE adatoms and O atoms on the (001) surface of kaolinite. (Dif. = After – Before, —> (+) win e−, (−) lost e−).

Site	Y	Y			Nd			La		
		Before	After	Dif.	Before	After	Dif.	Before	After	Dif.
Top	Y (Nd or La)	11	10.68	−0.32	14	13.68	−0.32	11	10.46	−0.54
	O ₁	1.43	1.48	0.05	1.43	1.47	0.04	1.43	1.46	0.03
Bridge	Y (Nd or La)	11	10.54	−0.46	14	13.51	−0.49	11	10.58	−0.42
	O ₂	1.43	1.45	0.02	1.52	1.53	0.01	1.46	1.53	0.07
	O ₃	1.52	1.56	0.04	1.47	1.55	0.08	1.50	1.51	0.01
	Y (Nd or La)	11	10.55	−0.45	14	13.30	−0.70	11	10.29	−0.71
Hollow	O ₄	1.52	1.54	0.02	1.46	1.52	0.06	1.52	1.59	0.07
	O ₅	1.44	1.46	0.02	1.48	1.50	0.02	1.45	1.48	0.03
	O ₆	1.43	1.44	0.01	1.45	1.47	0.02	1.46	1.48	0.02

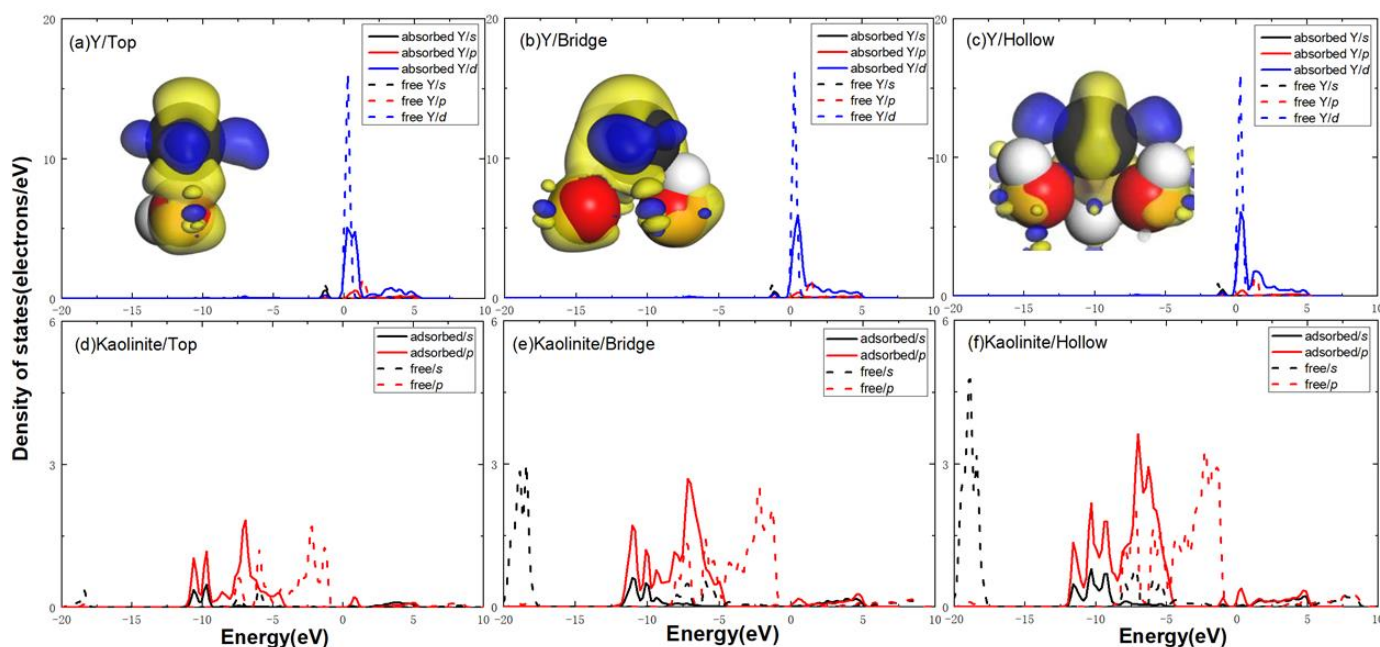


Figure 3. The PDOS plots for the Y and the neighboring O atoms bonded to Y at the stable top, bridge, and hollow adsorption sites on (001) surface: (a–c) free and adsorbed Y at the top, bridge, and hollow adsorption site, respectively; (d–f) clean and adsorbed kaolinite (001) surface at the top, bridge, and hollow adsorption site, respectively. The insets show the side view of electron density difference for the Y at the top, bridge, and hollow adsorption sites.

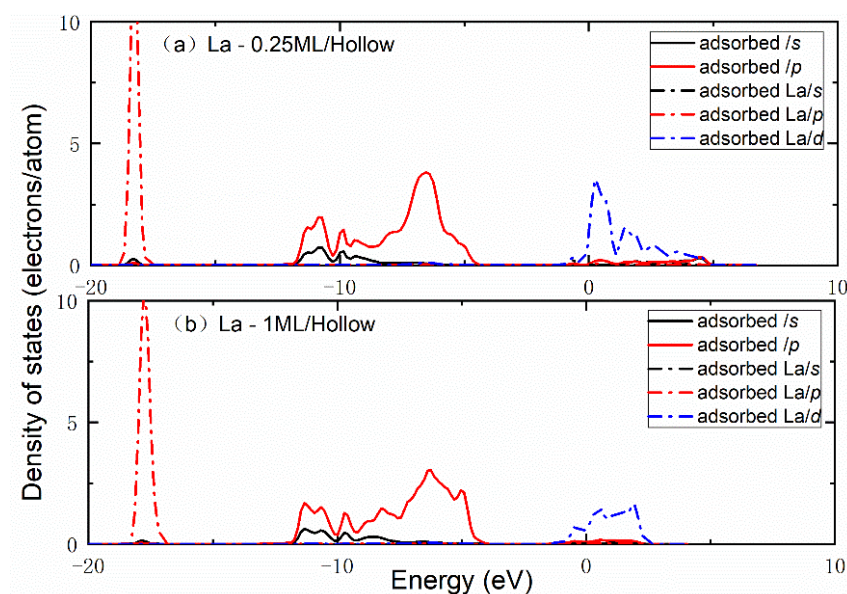


Figure 4. The PDOS of La atoms adsorbed at a hollow site and neighboring atoms of kaolinite (001) surface with a coverage of 0.25 ML (a) and 1.0 ML (b).

We studied the chemisorption mechanism of REE atoms binding on the kaolinite surface further. As a typical case, the PDOS at the three adsorption sites of the corresponding adjacent O and H atoms on the surface of Y and kaolinite (001) before and after adsorption were also calculated, as shown in Figure 3. Comparing the PDOS of the free and the adsorbed state Y, it can be clearly seen that the orbital peak energy of the adsorbed Y atom is significantly lower and broader than that of the free state, and the energy band of the adsorbed Y atom moved to a lower area and dropped by 0.3, 0.2, and 0.2 eV, respectively, relative to the Fermi surface. When Y was adsorbed on the top sites, the orbital energy of *d* decreased by 0.93 eV. At the same time, new peaks appeared in the *s* and *p* orbitals of the H and O atoms of kaolinite (001), which aligned with the *p* bonding orbital of adsorbed Y in the energy range from 0.54 to 1.23 eV (Figure 3a,d). The above results showed that the lone pair electron of the adsorbed Y atom overlapped with the O 2*p* orbit and formed a Y–O covalent bond. As shown in Figure 4b, after the Y atom was adsorbed at the bridge site, the *s* orbital decreased by 0.96 eV, and the peak density of the *s*, *p*, *d* orbital state was lower than that of the top site and hollow site. The energy overlapped between the adsorbed Y and the surface of kaolinite (001) in the range of 1.29–5.15 eV. As shown in the inset in Figure 3b, a Y atom provided electrons to the two O atoms on the surface of kaolinite, forming two covalent bonds. Similarly, when the Y atom was adsorbed at the hollow site, three oxygen bonds were formed.

Figure 4a,b show the PDOS of the most stable REE—La—adsorbed at the hollow site of the kaolinite (001) surface at $\Theta = 0.25$ and $\Theta = 1.0$ ML in order to understand the difference between adsorbing single and multiple REE atoms. Comparing the PDOS of La atoms with coverages of 0.25 ML and 1.0 ML, it can be clearly seen that the high coverage Y atom *p* and *d* orbitals were significantly lower and wider than the peak value of a low coverage Y atom. Moreover, the *d* orbital energy of the adsorbed La atom was reduced by 0.53 eV relative to the Fermi surface. On the other hand, the *s* and *p* orbital energies of H and O atoms moved to lower energy directions, and the *p* orbital of the O atom divided into several small peaks at -9.7 – -2.3 eV, showing its non-locality, which indicated that the La atom has strong chemical adsorption on the surface of kaolinite. These characteristics indicated that when multiple La atoms were adsorbed, the *p* and *d* orbitals had more charge transfer and the mutual adsorption was stronger, indicating that the La atoms were more inclined to bind with the O atoms on the surface of kaolinite, and the covalent properties of La–O increased with the increase in the coverage.

4. Conclusions

In this paper, the adsorption mechanism and geometric configuration of REE atoms on kaolinite (001) and (00 $\bar{1}$) surfaces, as well as the binding positions, binding energies, and the electron transfer, were investigated by the density functional theory. Compared with the E_{ads} of REEs adsorbed on (001) and (00 $\bar{1}$) surfaces of kaolinite, REE atoms were more likely to be adsorbed near the hydroxyl groups on the (001) surface of kaolinite, and we found that the best adsorption site on the kaolinite (001) surface was the bridge site for Y atoms, and the hollow site was the favorite adsorption site for Nd and La atoms. Meanwhile, the hollow site of the kaolinite (00 $\bar{1}$) surface was found to be energetically preferred for Y and Nd atoms, while the bridge site was the most stable adsorption site for La atoms. Furthermore, the adsorption behavior of Y, Nd, and La atoms on the kaolinite (001) surface with different coverages was investigated. According to the above discussion, REE atoms were mainly adsorbed on the (001) surface of kaolinite through covalent interaction, and the interaction between REE atoms increased with the increasing of Θ values. The adsorption energy of Y, Nd, and La atoms on three kinds of sites increased with increasing of the coverage implied the stronger capability of surface adsorption. The recovery capability of kaolinite for rare earth atoms was in the order of La > Nd > Y. The above results are of great significance to theoretical studies of the adsorption mechanism of rare earth atoms on kaolinite (001) and (00 $\bar{1}$) surfaces, which lays a solid foundation for the recovery and utilization of REEs.

Supplementary Materials: The following are available online at <https://www.mdpi.com/article/10.3390/min11080856/s1>, Figure S1: Structural model of Nd atom adsorbed at top site with increasing of the coverage range.

Author Contributions: Conceptualization and methodology, J.Z.; software, J.Z.; validation, formal analysis, data curation, and writing, J.Z., Z.W., W.G.; investigation, J.Z., Y.-F.W., B.-W.H. All authors have read and agreed to the published version of the manuscript.

Funding: This research was funded by the National Natural Science Foundation of China (No. 41702317), the Fundamental Research Funds for the central universities, and the National Training Program of Innovation and Entrepreneurship for undergraduates.

Conflicts of Interest: The authors declare no conflict of interest.

References

1. Ogata, T.; Narita, H.; Tanaka, M. Adsorption behavior of rare earth elements on silica gel modified with diglycol amic acid. *Hydrometallurgy* **2015**, *152*, 178–182. [[CrossRef](#)]
2. Greaves, M.; Elderfield, H.; Sholkovitz, E. Aeolian sources of rare earth elements to the Western Pacific Ocean. *Mar. Chem.* **1999**, *68*, 31–38. [[CrossRef](#)]
3. Voßenkaul, D.; Stoltz, N.; Meyer, F.M.; Friedrich, B. Extraction of Rare Earth Elements from non-Chinese Ion Adsorption Clays. In Proceedings of the European Metallurgical Conference (EMC), Düsseldorf, Germany, 14–17 June 2015. [[CrossRef](#)]
4. Anastopoulos, I.; Bhatnagar, A.; Lima, E.C. Adsorption of rare earth metals: A review of recent literature. *J. Mol. Liq.* **2016**, *221*, 954–962. [[CrossRef](#)]
5. Kondo, K.; Kamio, E. Separation of rare earth metals with a polymeric micro-capsule membrane. *Desalination* **2002**, *144*, 249–254. [[CrossRef](#)]
6. Araki, K.; Yoshida, M.; Uezu, K.; Goto, M.; Furusaki, S. Lanthanide-Imprinted Resins Prepared by Surface Template Polymerization. *J. Chem. Eng. Jpn.* **2000**, *33*, 665–668. [[CrossRef](#)]
7. Alakhras, F.; Abu Dari, K.; Mubarak, M.S. Synthesis and chelating properties of some poly(amidoxime-hydroxamic acid) resins toward some trivalent lanthanide metal ions. *J. Appl. Polym. Sci.* **2005**, *97*, 691–696. [[CrossRef](#)]
8. Choi, S.-H.; Lee, K.-P.; Sohn, S.-H. Graft copolymer-lanthanide complexes obtained by radiation grafting on polyethylene film. *J. Appl. Polym. Sci.* **2002**, *87*, 328–336. [[CrossRef](#)]
9. Chen, Y.G.; Zhu, B.H.; Wu, D.B.; Wang, Q.G.; Yang, Y.H.; Ye, W.M.; Guo, J.F. Eu(III) adsorption using di(2-ethylhexyl) phosphoric acid-immobilized magnetic GMZ bentonite. *Chem. Eng. J.* **2012**, *181*, 387–396. [[CrossRef](#)]
10. Iannicelli-Zubiani, E.M.; Cristiani, C.; Dotelli, G.; Stampino, P.G.; Pelosato, R.; Mesto, E.; Schingaro, E.; Lacalamita, M. Use of natural clays as sorbent materials for rare earth ions: Materials characterization and set up of the operative parameters. *Waste Manag.* **2015**, *46*, 546–556. [[CrossRef](#)]

11. Moldoveanu, G.A.; Papangelakis, V.G. Recovery of rare earth elements adsorbed on clay minerals: I. Desorption mechanism. *Hydrometallurgy* **2012**, *117*, 71–78. [[CrossRef](#)]
12. Moldoveanu, G.A.; Papangelakis, V.G. Recovery of rare earth elements adsorbed on clay minerals: II. Leaching with ammonium sulfate. *Hydrometallurgy* **2013**, *131*, 158–166. [[CrossRef](#)]
13. Chegrouche, S.; Mellah, A.; Telmoune, S. Removal of lanthanum from aqueous solutions by natural bentonite. *Water Res.* **1997**, *31*, 1733–1737. [[CrossRef](#)]
14. Chen, Y.; Zhu, C.; Sun, Y.; Duan, H.; Ye, W.; Wu, D. Adsorption of La(III) onto GMZ bentonite: Effect of contact time, bentonite content, pH value and ionic strength. *J. Radioanal. Nucl. Chem.* **2012**, *292*, 1339–1347. [[CrossRef](#)]
15. Chen, Y.H.; Lu, D.L. H₂ capture by kaolinite and its adsorption mechanism. *Appl. Clay Sci.* **2015**, *104*, 221–228. [[CrossRef](#)]
16. Brigatti, M.F.; Galan, E.; Theng, B.K.G. Handbook of Clay Science. In *General Introduction: Clays Clay Minerals, and Clay Science*; Bergaya, F., Theng, B.K.G., Lagaly, G., Eds.; Elsevier Ltd: Amsterdam, The Netherlands, 2006; pp. 27–30.
17. Laufer, F.; Yariv, S.; Steinberg, M. The adsorption of quadrivalent cerium by kaolinite. *Clay Miner.* **1984**, *19*, 137–149. [[CrossRef](#)]
18. Aja, S.U. The Sorption of the Rare Earth Element, Nd, onto Kaolinite at 25 °C. *Clays Clay Miner.* **1998**, *46*, 103–109. [[CrossRef](#)]
19. Coppin, F.; Berger, G.; Bauer, A.; Castet, S.; Loubet, M. Sorption of lanthanides on smectite and kaolinite. *Chem. Geol.* **2002**, *182*, 57–68. [[CrossRef](#)]
20. Wan, Y.; Liu, C. The effect of humic acid on the adsorption of REEs on kaolin. *Colloids Surf. A Physicochem. Eng. Asp.* **2006**, *290*, 112–117. [[CrossRef](#)]
21. Xiao, Y.; Huang, L.; Long, Z.; Feng, Z.; Wang, L. Adsorption ability of rare earth elements on clay minerals and its practical performance. *J. Rare Earths* **2016**, *34*, 543–548. [[CrossRef](#)]
22. He, M.-C.; Zhao, J. Effects of Mg, Ca, and Fe(II) Doping on the Kaolinite (001) Surface with H₂O Adsorption. *Clays Clay Miner.* **2012**, *60*, 330–337. [[CrossRef](#)]
23. Zhao, J.; Wang, J.; Qin, X.; Cao, Y. An ab-initio study of H₂O adsorption on the calcite (104) surface with different coverages. *Solid State Commun.* **2020**, *313*, 113892. [[CrossRef](#)]
24. Zhang, Z.; Zhou, Q.; Zhuang, L.; Zhao, Z. Adsorption of Ca(II) and K(I) on the kaolinite surface: A DFT study with an experimental verification. *Mol. Phys.* **2021**, *119*, e1896047. [[CrossRef](#)]
25. Hou, J.L.; Chen, M.; Zhou, Y.F.; Bian, L.; Dong, F.Q.; Tang, Y.H.; Ni, Y.X.; Zhang, H.P. Regulating the effect of element doping on the CO₂ capture performance of kaolinite: A density functional theory study. *Appl. Surf. Sci.* **2020**, 512. [[CrossRef](#)]
26. Kuriki, K.; Koike, Y.; Okamoto, Y. Plastic Optical Fiber Lasers and Amplifiers Containing Lanthanide Complexes. *Chem. Rev.* **2002**, *102*, 2347–2356. [[CrossRef](#)] [[PubMed](#)]
27. Hull, R.; Parisi, J.; Osgood, R.M. *Spectroscopic Properties of Rare Earths in Optical Materials Volume 83: Rare Earth Ions in Advanced X-ray Imaging Materials*; Springer Series in Materials Science; Springer: Berlin/Heidelberg, Germany, 2005; Chapter 10, pp. 500–529.
28. Zou, J.H.; Liu, D.; Tian, H.M.; Liu, F.; Li, T.; Yang, H.Y. Geochemical characteristics of trace elements and rare earth elements of Late Paleozoic Coal in Adahai mine, Inner Mongolia. *Acta Coalae Sin.* **2013**, *38*, 12–1018. (In Chinese)
29. Kresse, G.; Furthmüller, J. Efficient iterative schemes for ab initio total-energy calculations using a plane-wave basis set. *Phys. Rev. B* **1996**, *54*, 11169–11173. [[CrossRef](#)]
30. Blöchl, P.E. Projector augmented-wave method. *Phys. Rev. B* **1994**, *50*, 17953–17979. [[CrossRef](#)]
31. Adams, J.M. Hydrogen Atom Positions in Kaolinite by Neutron Profile Refinement. *Clays Clay Miner.* **1983**, *31*, 352–356. [[CrossRef](#)]
32. Bish, D.L. Rietveld Refinement of the Kaolinite Structure at 1.5 K. *Clays Clay Miner.* **1993**, *41*, 738–744. [[CrossRef](#)]
33. Benco, L.; Tunega, D.; Hafner, J.; Lischka, H. Orientation of OH groups in kaolinite and dickite: Ab initio molecular dynamics study. *Am. Miner.* **2001**, *86*, 1057–1065. [[CrossRef](#)]
34. Bailey, S.W. Structure of layer silicates. In *Crystal Structures of Clay Minerals and Their X-Ray Identification*; Brindley, G.W., Brown, G., Eds.; Mineralogical Society: London, UK, 1980; pp. 36–123.
35. Hayashi, S. NMR Study of Dynamics and Evolution of Guest Molecules in Kaolinite/Dimethyl Sulfoxide Intercalation Compound. *Clays Clay Miner.* **1997**, *45*, 724–732. [[CrossRef](#)]
36. Hess, A.C.; Saunders, V.R. Periodic ab initio Hartree-Fock calculations of the low-symmetry mineral kaolinite. *J. Phys. Chem.* **1992**, *96*, 4367–4374. [[CrossRef](#)]
37. Hobbs, J.D.; Schultz, P.A.; Sears, M.P.; Cygan, R.T.; Nagy, K.L. All-atom ab initio energy minimization of the kaolinite crystal structure. *Am. Miner.* **1997**, *82*, 657–662. [[CrossRef](#)]
38. Hu, X.L.; Angelos, M. Water on the hydroxylated (001) surface of kaolinite: From monomer adsorption to a flat 2D wetting layer. *Surf. Sci.* **2008**, *602*, 960–974. [[CrossRef](#)]
39. Plancon, A.; Giese Jr, R.F.; Snyder, R.; Drits, V.A.; Bookin, A.S. Stacking faults in the kaolinite-group minerals: Defect structures of kaolinite. *Clays Clay Miner.* **1997**, *37*, 195–198. [[CrossRef](#)]
40. Teppen, B.J.; Rasmussen, K.; Bertsch, P.; Miller, D.M.; Schäfer, L. Molecular Dynamics Modeling of Clay Minerals. 1. Gibbsite, Kaolinite, Pyrophyllite, and Beidellite. *J. Phys. Chem. B* **1997**, *101*, 1579–1587. [[CrossRef](#)]
41. Schwieger, W.; Lagaly, G.; Dutta, P.; Auerbach, S.; Carrad, K. Alkali Silicates and Crystalline Silicic Acids. In *Handbook of Layered Materials*; Informa UK Limited: London, UK, 2004; pp. 541–629.
42. Sato, H.; Ono, K.; Johnston, C.T.; Yamagishi, A. First-principles studies on the elastic constants of a 1:1 layered kaolinite mineral. *Am. Miner.* **2005**, *90*, 1824–1826. [[CrossRef](#)]

43. Kresse, G.; Joubert, D. From ultrasoft pseudopotentials to the projector augmented-wave method. *Phys. Rev. B* **1999**, *59*, 1758–1775. [[CrossRef](#)]
44. Zhao, J.; He, M.-C. Theoretical study of heavy metal Cd, Cu, Hg, and Ni(II) adsorption on the kaolinite (001) surface. *Appl. Surf. Sci.* **2014**, *317*, 718–723. [[CrossRef](#)]
45. Chi, R.A.; Wang, D.Z. Quantum chemical calculation of adsorption properties of clay minerals and enrichment of rare earths. *Chin. J. Rare Earths* **1993**, *4*, 199–203. (In Chinese)
46. Zhao, J.; Gao, W.; Qin, X.Z. First-principles study on adsorption behavior of as on the kaolinite (001) and (001) surfaces Adsorption. *Adsorption* **2020**, *26*, 443–452. [[CrossRef](#)]